

SUSY after the 125 GeV Higgs Discovery

PN

Northeastern University, Boston, MA 02115

KITP Santa Barbara, May 2013

Contents

- Brief intro on SUSY
- The 125 GeV Higgs mass points to a high SUSY scale.
- Conflicting data
 - From Brookhaven on $g_{\mu} - 2$ with a 3σ deviation from SM points to a low scale SUSY.
 - Fledgling excess in Higgs to 2 gamma decay also points to a low scale SUSY.
- Possible resolutions
 - SUGRA unification with nonuniversalities.
 - Lower the SUSY scale.
- Additional topics
 - High Higgs boson mass and hyperbolic geometry of REWSB.
 - Connection of the Higgs mass to proton stability.
 - Naturalness and fine tuning

Brief intro to SUSY

- SUSY is an extension of the space time symmetry. It is primarily a high scale symmetry.
- The Wess-Zumino 4-dim SUSY¹ is a global symmetry and difficult to break in a phenomenologically viable fashion.
- Gauging of SUSY brings in gravity ² and leads to supergravity³.

¹J. Wess, B. Zumino, Nucl.Phys. B70 (1974) 39-50; Phys.Lett. B49 (1974) 52

²PN, R. Arnowitt, Phys.Lett. B56 (1975) 177
R. Arnowitt, PN, B. Zumino, Phys.Lett. B56 (1975)81.

³D Z Freedman, P. van Nieuwenhuizen, S. Ferrara, Phys.Rev. D13 (1976) 3214-3218.

SUSY Unification

- Models based on SUSY help resolve the hierarchy problem but again SUSY breaking is a problem⁴
- Supergravity grand unification (SUGRA) breaks SUSY via gravity mediation.⁵ It depends on three arbitrary functions⁶

$$K(z, z^\dagger), W(z), f_{\alpha\beta}$$

- Under simplifying assumptions on K and $f_{\alpha\beta}$ the parameter space is⁷

$$m_0, m_{1/2}, A_0, B_0, \mu_0$$

- Under radiative breaking of the electroweak symmetry⁸ one can redefine the parameter space of the universal SUGRA models

$$m_0, m_{1/2}, A_0, \tan \beta, \text{sign}(\mu).$$

⁴S. Dimopoulos and H. Georgi, Nucl.Phys. B193 (1981) 150

⁵A H Chamseddine, R. Arnowitt, PN, Phys.Rev.Lett. 49 (1982) 970

⁶PN, R Arnowitt, A H Chamseddine, Applied N=1 Supergravity, ICTP Lecture Series 1983; E. Cremmer, S. Ferrara, L. Girardello and A. Van Proeyen, Nucl. Phys. B **212**, 413 (1983).

⁷PN, R. L. Arnowitt and A. H. Chamseddine, Nucl. Phys. B **227**, 121 (1983).
L. J. Hall, J. D. Lykken and S. Weinberg, Phys. Rev. D **27**, 2359 (1983).

⁸L. Alvarez-Gaume, J. Polchinski and M. B. Wise, Nucl. Phys. B **221**, 495 (1983);
L. E. Ibanez and C. Lopez, Phys. Lett. B128, 54 (1983).

SUSY unification-2

- SUGRA GUTS allows for nonuniversalities in the soft parameters, via choices of the Kahler potential and for the gauge kinetic energy function. These lead to
 - NuSUGRA: This has non-universalities in the gaugino sector.
 - NUHM: nonuniversalities in the Higgs sector.
 - cSUGRA; Soft parameters are allowed to have phases.
 - SUGRA with flavor: For example, the third generation soft masses may be different.

There are other possibilities for breaking of SUSY

- Gauge mediation ⁹
- Anomaly mediation ¹⁰

⁹M. Dine, A. E. Nelson, Phys. Rev. D **48**, 1277 (1993); Early work: M. Dine, W. Fischler and M. Srednicki, Nucl. Phys. B **189**, 575 (1981).

¹⁰L. Randall and R. Sundrum, Nucl. Phys. B **557**, 79 (1999); G. F. Giudice, M. A. Luty, H. Murayama and R. Rattazzi, JHEP **9812**, 027 (1998).

SUSY unification -3

Low energy limit of string models and of brane models is $\mathcal{N} = 1$ supergravity. Thus supergravity models encompass a broad class, the various models being discriminated by the choices of the Kahler potential, the superpotential and the gauge kinetic energy function.

The LHC constraints on the sugra models with universal boundary conditions

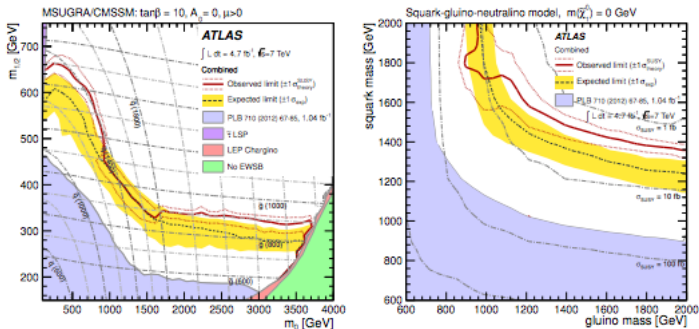
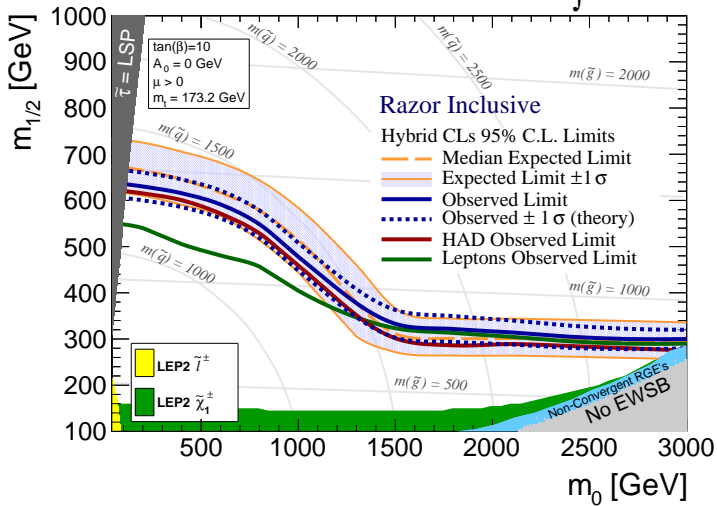


Figure 1: Exclusion plots in the MSUGRA/CMSSM (left) and squark-gluino-neutralino (right) models from Ref. [2].

CMS $\sqrt{s} = 7 \text{ TeV}$ $\int L dt = 4.7 \text{ fb}^{-1}$



Higgs boson discovery

- ATLAS and CMS Collaborations have measured the mass of a new boson which lies between 125 and 126 GeV¹¹. While many properties of the new boson need still to be identified it is the general belief that the particle seen is the Higgs boson which enters in the electroweak symmetry breaking
- It is quite remarkable that the observed Higgs boson mass lies close to the upper limit predicted in grand unified supergravity models which is roughly 130 GeV^{12, 13, 14}.

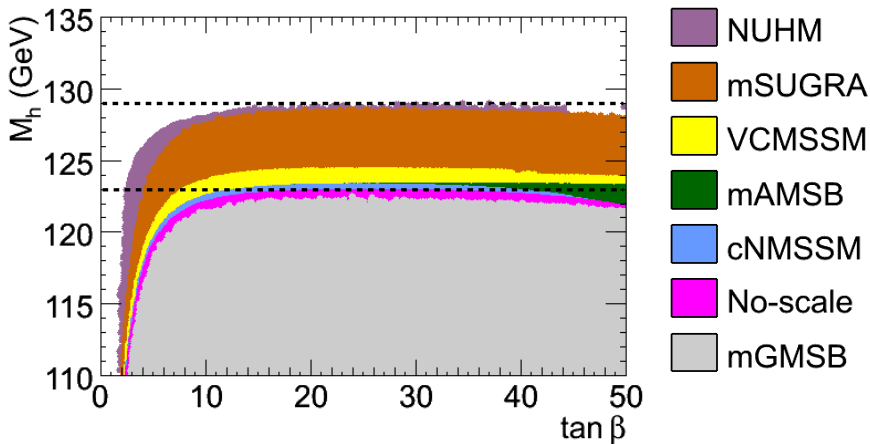
¹¹CMS Collaboration, Phys. Lett. B, 716, (2012) 30–61, arXiv:1207.7235
ATLAS Collaboration, Phys. Lett. B, 716 (2012) 1–29. arXiv:1207.7214.

¹²S. Akula, B. Altunkaynak, D. Feldman, PN and G. Peim, PRD **85**, 075001 (2012).

¹³A. Arbey, M. Battaglia, A. Djouadi and F. Mahmoudi, JHEP 1209 (2012) 107, arXiv:1207.1348 [hep-ph].

¹⁴O. Buchmueller, R. Cavanaugh, A. De Roeck et al. Eur. Phys. J. C 72 (2012) 2020, arXiv:1112.3564.

A comparison of mSUGRA, mGMSB, mAMSB and others



A. Arbey, M. Battaglia, A. Djouadi and F. Mahmoudi, JHEP 1209 (2012) 107,
arXiv:1207.1348 [hep-ph].

No-scale: $m_0 \approx A_0 \approx 0$

cNMSSM: $m_0 \approx 0, A_0 \approx -\frac{1}{4}m_{1/2}$

VCMSSM: $A_0 \approx -m_0$

NUHM: mSUGRA + two more inputs.

**A. Arbey, M. Battaglia, A. Djouadi, F. Mahmoudi and J. Quevillon, Phys.Lett.
B708 (2012) 162-169, arXiv:1112.3028.**

Implications of the ~ 125 GeV Higgs boson

- SM: Within the standard model the Higgs is a bit too light.
- SUSY: Within SUSY the Higgs is a bit too heavy.

~ 125 GeV Higgs boson in SM

In the Standard Model vacuum stability puts a stringent constraint on the allowed range of the Higgs mass.

- With the inclusion of both the theoretical error in the evaluation of m_h estimated at ± 1.0 GeV and the experimental errors on the top mass and α_s the analysis¹⁵

$$m_h > 129.4 \pm 1.8 \text{ GeV},$$

for the standard model to have vacuum stability up to the Planck scale. This excludes the vacuum stability for the SM for $m_{h0} < 126$ GeV at the 2σ level.

- The Higgs mass of ~ 125 GeV would give vacuum stability up to only scales between $10^9 - 10^{10}$ GeV and stability up to the Planck scale would require new physics.
- Vacuum stability is less problematic in supersymmetric theories¹⁶

¹⁵Degrassi, Di Vita, Elias-Miro, Espinosa, Giudice et al. JHEP, 1208, 098 (2012).

¹⁶J. Hisano and S. Sugiyama, Phys.Lett. B696, 92 (2011), arXiv:1011.0260 [hep-ph].

. Carena, S. Gori, I. Low, N. R. Shah and C. E. Wagner, JHEP 1302, 114 (2013), T. Kitahara, JHEP 1211, 021 (2012), arXiv:1208.4792 [hep-ph].

A Higgs mass ~ 125 GeV implies a high SUSY scale

- In MSSM the Higgs boson mass obeys at the tree level

$$m_h < M_Z$$

and a large loop correction is needed to pull it up the experimental value.

- The dominant one loop contribution arises from the top/stop sector and is given by

$$\Delta m_h^2 \simeq \frac{3m_t^4}{2\pi^2 v^2} \ln \frac{M_S^2}{m_t^2} + \frac{3m_t^4}{2\pi^2 v^2} \left(\frac{X_t^2}{M_S^2} - \frac{X_t^4}{12M_S^4} \right) + \dots$$

$v = 246$ GeV (v is the Higgs VEV), M_S is an average stop mass, and $X_t \equiv A_t - \mu \cot \beta$.

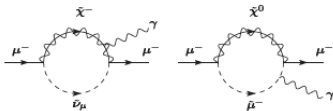
- An $m_h \sim 125$ GeV implies M_S in the several TeV region.

Conflicting evidence from muon anomalous moment

- The Brookhaven experiment E821¹⁷ which measures $a_\mu = \frac{1}{2}(g_\mu - 2)$ shows a deviation from the Standard Model prediction¹⁸ at the 3σ level.

$$\delta a_\mu = (287 \pm 80.) \times 10^{-11}. \quad (1)$$

The SUSY contribution¹⁹ arises from $\tilde{\chi}^\pm - \tilde{\nu}_\mu$ and $\tilde{\chi}_1^0 - \tilde{\mu}$ loops.



A rough estimate of the supersymmetric correction is

$$\delta a_\mu \simeq \text{sign}(\mu) \left(130 \times 10^{-11}\right) \left(\frac{100 \text{ GeV}}{M_{\text{SUSY}}}\right)^2 \tan \beta. \quad (2)$$

- In order to obtain a SUSY correction of size indicated by the Brookhaven experiment masses of sparticles in the loops, i.e., the masses of $\tilde{\chi}^\pm$, $\tilde{\nu}_\mu$, $\tilde{\chi}_1^0$, $\tilde{\mu}$ must be only about a few hundred GeV.

¹⁷ Muon G-2 Collaboration, Phys. Rev. D 73 (2006) 072003

¹⁸ K. Hagiwara, R. Liao, A. D. Martin et al. J. Phys. G, 38 (2011) 085003, M. Davier, A. Hoecker, B. Malaescu et al. Eur. Phys. J. C, 71 (2011) 1515.

¹⁹ T. Yuan, R. L. Arnowitt, A. H. Chamseddine, P.N., Z. Phys. C, 26 (1984) 407; D. A. Kosower, L. M. Krauss, and N. Sakai, Phys. Lett. B 133 (1983) 305; S. Heinemeyer, D. Stockinger, and G. Weiglein, Nucl. Phys. B 690 (2004) 62-80.

Higgs to diphoton rate

Another indication of low scale for SUSY

There is a possible excess in the Higgs to diphoton decay. The ATLAS²⁰ and CMS²¹ Collaborations give

$$R_{\gamma\gamma} \equiv \frac{\sigma(pp \rightarrow h)_{\text{obs}}}{\sigma(pp \rightarrow h)_{\text{SM}}} \cdot \frac{\Gamma(h \rightarrow \gamma\gamma)_{\text{obs}}}{\Gamma(h \rightarrow \gamma\gamma)_{\text{SM}}} = 1.8 \pm 0.5 \text{ (ATLAS)}, 1.6 \pm 0.4 \text{ (CMS)},$$

where

$$\frac{\sigma(pp \rightarrow h)_{\text{obs}}}{\sigma(pp \rightarrow h)_{\text{SM}}} = 1.4 \pm 0.3 \text{ (ATLAS)}, 0.87 \pm 0.23 \text{ (CMS)}. \quad (4)$$

²⁰G. Aad et al. [ATLAS Collaboration], Phys. Lett. B 716, 1 (2012).

²¹S. Chatrchyan et al. [CMS Collaboration], Phys. Lett. B 716, 30 (2012).

Some possible resolutions

- Regarding $g_{\mu} - 2$ perhaps we do not understand the hadronic corrections. In the past the evaluation of the hadronic correction has shifted. Perhaps more accurate determination of hadronic and experimental errors might remove the discrepancy. May be the diphoton excess is due to QCD uncertainties.

But suppose we take the BNL result at face value and assume also that the diphoton excess will persist. In that case we need some modification of the standard paradigm. I will consider two possibilities:

- **Path I:**

One possibility is within gluino driven radiative breaking where the gluino mass is taken to be much larger than other soft masses. This model leads to a split scale SUSY, with a low scale in the few hundred GeV region and a high scale which lies in the several TeV region.

- **Path II:**

As a second possibility we consider that there are contributions to the Higgs boson mass outside of MSSM. This extra contribution will allow to lower the SUSY scale and relieve the tension. It will also contribute to the diphoton rate of the Higgs.

Path I

SUGRA unification with unconventional boundary conditions at high scale

As mentioned the experimental evidence points to color particles being much heavier than the uncolored particles. Thus we specify the boundary conditions for soft parameters by ²²

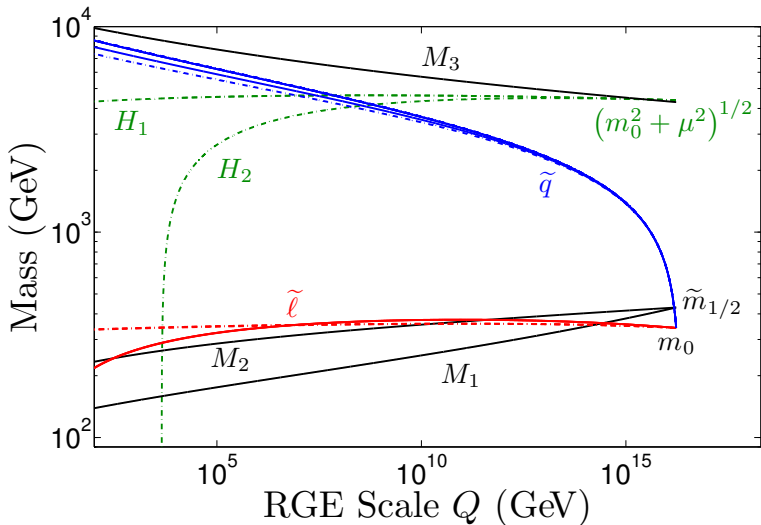
$$m_0, m_3, A_0, \tan \beta, \text{sign}(\mu)$$

while $m_1 = m_2 \ll m_3$. As illustrative example we choose $m_3/m_1 = 10$, $m_3 \gg m_0$. The renormalization group evolution of squarks is dominated by the gluino mass.

$$\frac{d}{dt} \begin{bmatrix} m_{H_2}^2 \\ m_U^2 \\ m_Q^2 \end{bmatrix} = -Y_t \begin{bmatrix} 3 & 3 & 3 \\ 2 & 2 & 2 \\ 1 & 1 & 1 \end{bmatrix} \begin{bmatrix} m_{H_2}^2 \\ m_U^2 \\ m_Q^2 \end{bmatrix} - Y_t A_t^2 \begin{bmatrix} 3 \\ 2 \\ 1 \end{bmatrix} + \begin{bmatrix} 3\tilde{\alpha}_2 m_2^2 + \tilde{\alpha}_1 m_1^2 \\ \frac{16}{3}\tilde{\alpha}_3 m_3^2 + \frac{16}{9}\tilde{\alpha}_1 m_1^2 \\ \frac{16}{3}\tilde{\alpha}_3 m_3^2 + 3\tilde{\alpha}_2 m_2^2 + \frac{1}{9}\tilde{\alpha}_1 m_1^2 \end{bmatrix}.$$

²² S. Akula and PN., "Gluino-driven Radiative Breaking, Higgs Boson Mass, Muon $g - 2$, and the Higgs Diphoton Decay in SUGRA Unification," arXiv:1304.5526 [hep-ph].

Split scale SUSY spectrum for \tilde{g} SUGRA.



Light and heavy spectrum of Split Scale SUSY

- Particles with light masses ²³

$$\chi_1^0, \chi_2^0, \chi_1^\pm, \tilde{\tau}_1, \tilde{\tau}_2, \tilde{l}$$

- Particles with heavy masses

$$\chi_3^0, \chi_4^0, \chi_2^\pm, H^0, A^0, H^\pm, \tilde{q}, \tilde{g}$$

²³As a comparison the light spectrum of 'split susy' (Arkani-Hamed, Dimopoulos, JHEP **0506**, 073 (2005)) consists of light Higgsinos $\tilde{H}_{u,d}$, \tilde{B} , \tilde{W} , \tilde{g} and one Higgs doublet but does not have light sfermions.

A high scale solution

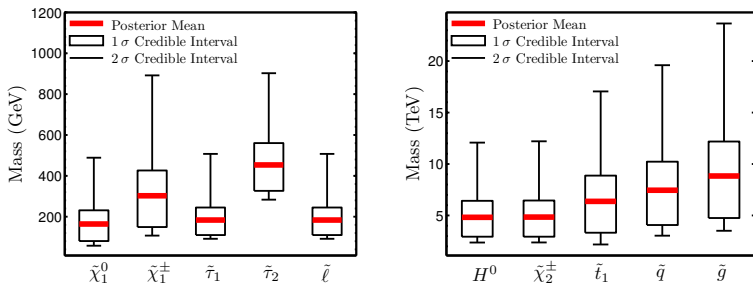


Figure: Split scale SUSY spectrum for \tilde{g} SUGRA.

Bayesian Posterior Probability Density

Define a set of input parameters²⁴ $\Theta = \{\theta, \psi\}$ so that

$$\theta = \{m_0, m_{1/2}, A_0, \tan \beta\}$$

$$\psi = \left\{ m_t, m_b(m_b)^{\overline{MS}}, \alpha_s(m_Z)^{\overline{MS}}, \alpha_{EM}(m_Z)^{\overline{MS}} \right\}.$$

ψ are referred to as nuisance parameters. Using Bayes's theorem, the posterior probability density function (PDF) for the theory described by Θ , which may be mapped to observables, $\xi(\Theta)$ to be compared against experimental data, d is given by:

$$p(\Theta|d) = \frac{p(d|\xi(\Theta))p(\Theta)}{p(d)}.$$

- $\mathcal{L}(\Theta) \equiv p(d|\xi(\Theta))$ is the likelihood function. For data which have experimental measurements, reported with uncertainties, the likelihood function is of the form

$$-2 \ln(\mathcal{L}(\Theta)) = \sum_i \frac{(\xi_i(\Theta) - d_i)^2}{\sigma_i^2 + \tau_i^2(\Theta)},$$

where σ_i represents in the total experimental uncertainty and τ_i estimates the theoretical uncertainty.

- $p(\Theta)$: It is the distribution in Θ prior to considering experimental results.
- $\mathcal{Z} \equiv p(d)$: It is the Bayesian evidence which can be used in model selection. However, in our goal of parameter estimation, it serves only as a normalization factor.

²⁴

See, F. Feroz, M. P. Hobson and M. Bridges, *Mon. Not. Roy. Astron. Soc.* **398**, 1601 (2009).

One then defines credible regions by $(1 - \alpha)$ where one defines an interval in θ_i , $[\theta_i^-, \theta_i^+]$ which satisfies

$$\int_{-\infty}^{\theta_i^-} d\theta_i P(\theta_i|D) = \alpha/2 \quad \text{and} \quad \int_{\theta_i^+}^{\infty} d\theta_i P(\theta_i|D) = \alpha/2 ,$$

where,

$$P(\theta_i|D) \equiv \int \prod_{j \neq i} d\theta_j \int \prod_k d\psi_k \mathcal{L}(\Theta, D) .$$

Thus if we wished to find the 95% credible region, we would set $\alpha = 0.05$.

Frequentist-style Profile Likelihood Ratio

In the profile likelihood ratio analysis, we take the test statistic to be the so-called *profile likelihood ratio*

$$\lambda(\theta) = \frac{\mathcal{L}(\theta, \hat{\psi})}{\mathcal{L}(\hat{\theta}, \hat{\psi})} .$$

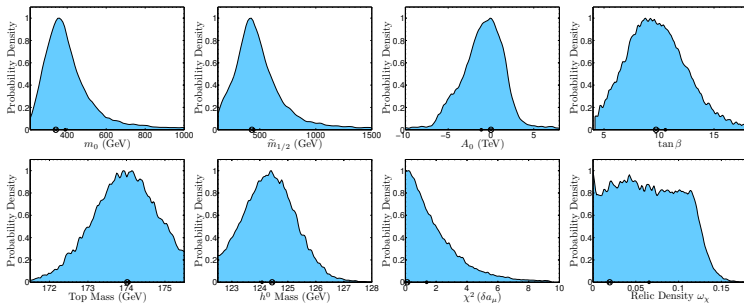
Here, $\mathcal{L}(\theta, \hat{\psi})$ is called the conditional maximal likelihood estimate (MLE), and $\mathcal{L}(\hat{\theta}, \hat{\psi})$ is called the unconditional MLE. These are defined by

$$\mathcal{L}(\theta, \hat{\psi}) = \max_{\psi} \mathcal{L}(\theta, \psi) \quad \text{and} \quad \mathcal{L}(\hat{\theta}, \hat{\psi}) = \max_{\theta, \psi} \mathcal{L}(\theta, \psi) .$$

The quantity $-2 \ln \mathcal{L}(\Theta)$ converges to a χ^2 distribution. Thus, one computes $\Delta\chi^2$ for a choice of $1 - \alpha$, and this gives the acceptance region.

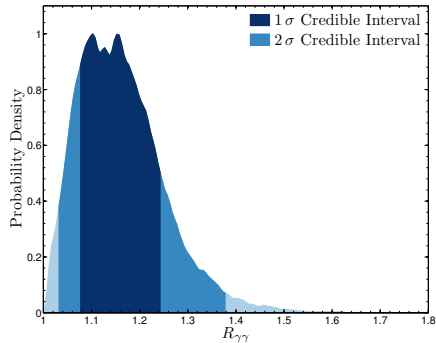
Observable	Central value	Exp. Err.	Th. Err.	Distribution	Ref.
SM Nuisance Parameters					
m_t	173.5 GeV	1.0 GeV	–	Gaussian	[13]
$m_b(m_b)^{\overline{MS}}$	4.18 GeV	0.03 GeV	–	Gaussian	[13]
$\alpha_s(m_Z)^{\overline{MS}}$	0.1187	7×10^{-4}	–	Gaussian	[13]
$1/\alpha_{EM}(m_Z)^{\overline{MS}}$	127.933	0.014	–	Gaussian	[13]
Measured					
$Br(B \rightarrow X_s \gamma) \times 10^4$	3.55	0.256	0.21	Gaussian	[15]
Ωh^2	0.1126	0.0036	10%	Upper-Gaussian	[14]
$m_{h,0}$	125.3 GeV	0.6 GeV	1.1 GeV	Gaussian	[1]
Limits (95% CL)					
$Br(B_s^0 \rightarrow \mu^+ \mu^-)$	4.5×10^{-9}	–	14%	Upper – Error Fn	[16]
$m_{h,0}$	122.5 GeV	–	–	Lower – Step Fn	[9]
$m_{h,0}$	129 GeV	–	–	Upper – Step Fn	[9]
$m_{\tilde{\chi}_1^0}$	46 GeV	–	5%	Lower – Error Fn	[13]
$m_{\tilde{\chi}_2^0}$	62.4 GeV	–	5%	Lower – Error Fn	[13]
$m_{\tilde{\chi}_3^0}$	99.9 GeV	–	5%	Lower – Error Fn	[13]
$m_{\tilde{\chi}_4^0}$	116 GeV	–	5%	Lower – Error Fn	[13]
$m_{\tilde{\chi}_1^\pm}$	94 GeV	–	5%	Lower – Error Fn	[13]
$m_{\tilde{g}_R}$	107 GeV	–	5%	Lower – Error Fn	[13]
$m_{\tilde{u}_R}$	94 GeV	–	5%	Lower – Error Fn	[13]
$m_{\tilde{t}_1}$	81.9 GeV	–	5%	Lower – Error Fn	[13]
$m_{\tilde{b}_1}$	89 GeV	–	5%	Lower – Error Fn	[13]
$m_{\tilde{t}_1}$	95.7 GeV	–	5%	Lower – Error Fn	[13]
$m_{\tilde{g}}$	500 GeV	–	5%	Lower – Error Fn	[13]
$m_{\tilde{g}}$	1100 GeV	–	5%	Lower – Error Fn	[13]

TABLE I: Summary of the observables used to estimate the mSUGRA parameters. Only the upper-half of the Gaussian is used in the consideration of Ωh^2 , i.e., there is only a penalty for values larger than the central value which allows for multicomponent dark matter [29]. The 95% CL limits have been evaluated under the assumption of only theoretical uncertainty, so the distribution used here is based on the error function, given explicitly in the fourth reference of [21].



A display of the marginalized posterior probability distributions for \tilde{g} SUGRA in the parameters of interest as well as some important derived quantities. The location of the best-fit point is indicated by a circled 'X' and the posterior mean is given with a solid dot.

Diphoton rate



Posterior probability density of $R_{\gamma\gamma}$ from our analysis. The 1σ and 2σ credible intervals are indicated in darker blues. We define $R_{\gamma\gamma}$ as the ratio of the diphoton partial width of the light CP -even Higgs boson to the corresponding width for a Standard Model Higgs of the same mass.

Possible signatures of \tilde{g} SUGRA at the LHC

- The observable sparticle spectrum at the LHC in this model consists of light sleptons and light electroweak gauginos.
- However, sleptons and electroweak gauginos are typically difficult to observe at the LHC and thus far have evaded detection in multi-lepton searches in experiments at the ATLAS and the CMS detectors with the 7 TeV and 8 TeV data. However, one expects that they would show up at higher energies and higher luminosities.
- The most promising $2 \rightarrow 2$ processes that can generate sparticles at the LHC in this model are

$$pp \rightarrow \tilde{\chi}_1^\pm \chi_1^\mp, \tilde{\chi}_2^0 \tilde{\chi}_1^\pm.$$

The identifying signatures of such processes will indeed be multi-leptons and missing energy.

Dark matter

The lightest neutralino is a possible candidate for dark matter in SUSY models²⁵. In SUGRA models an RG analysis confirms this to be the case over most of the parameter space of the model²⁶.

In general the neutralino is a linear combination of four fields, the bino, the wino and two higgsinos.

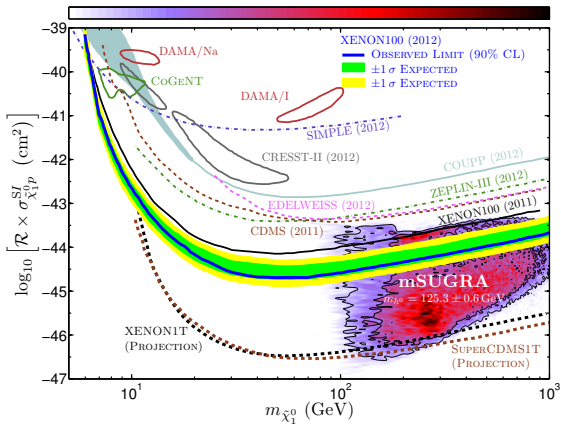
$$\chi^0 = \alpha \tilde{\lambda}_B + \beta \tilde{\lambda}_W + \gamma \tilde{H}_1 + \delta \tilde{H}_2^0.$$

The co-efficients $\alpha - \delta$ are very sensitive to the part of the parameter space one is in and the neutralino composition can vary from being purely bino, to purely wino to purely higgsino. The composition has important implications for the spin-independent dark matter cross-section.

²⁵ H. Goldberg, Phys. Rev. Lett. **50**, 1419 (1983); J. R. Ellis, J. S. Hagelin, D. V. Nanopoulos, K. A. Olive and M. Srednicki, Nucl. Phys. B **238**, 453 (1984).

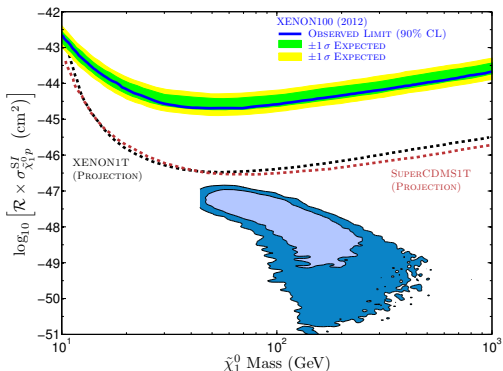
²⁶ R. L. Arnowitt and PN, Phys. Rev. Lett. **69**, 725 (1992).

Dark matter in mSUGRA under the Higgs boson mass of 125 GeV constraint



S. Akula, PN, arXiv:1210.0520 [hep-ph].

Dark matter in \tilde{g} SUGRA model ²⁷



S. Akula and PN, arXiv:1304.5526 [hep-ph].

A display of the 1σ and 2σ credible regions of the marginalized posterior PDF of \tilde{g} SUGRA in the plane of the spin-independent $p\text{-}\tilde{\chi}_1^0$ cross section and the $\tilde{\chi}_1^0$ mass. The current limit from XENON100 is displayed as well as the projected sensitivities for XENON1T and SuperCDMS1T.

High Higgs boson mass points to a hyperbolic geometry for REWSB

- In general the radiative breaking of the electroweak symmetry takes on the following form²⁸.

$$\mu^2 = \begin{pmatrix} +1 & (\text{EB}) \\ 0 & \\ -1 & (\text{HB}) \end{pmatrix} m_0^2 |C_1| + \Delta^2(m_{1/2}, A_0, \tan \beta),$$

where Δ^2 is a function of $m_{1/2}, A_0, \tan \beta$ and is positive.

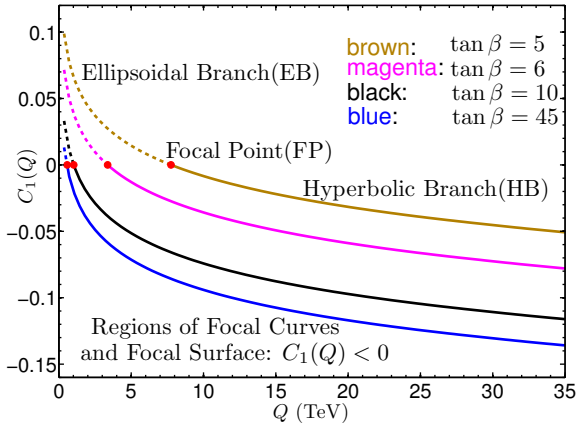
- The signs (\pm) are determined by the sign of $C_1(Q)$ with depends the renormalization group scale Q . The RG scale Q is chosen so that the two loop correction to the scalar potential is minimized. Typically $Q \sim M_S$ where $M_S = \sqrt{m_{\tilde{t}_1} m_{\tilde{t}_2}}$. A large correction to the Higgs boson requires that M_S lie in the several TeV range. This leads to

$$C_1(Q \sim M_S) < 0.$$

- Thus the large Higgs boson mass points to a Hyperbolic Geometry of REWSB.

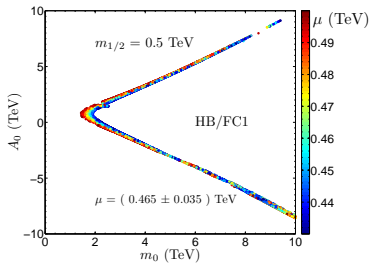
Regions of EB, HB .

Akula, Liu, PN, Peim, PLB 709, 192 (2012), arXiv:1111.4589 [hep-ph]

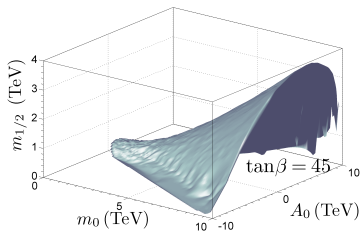


Focal curves and focal surfaces of hyperbolic geometry

Focal curves HB/FC1

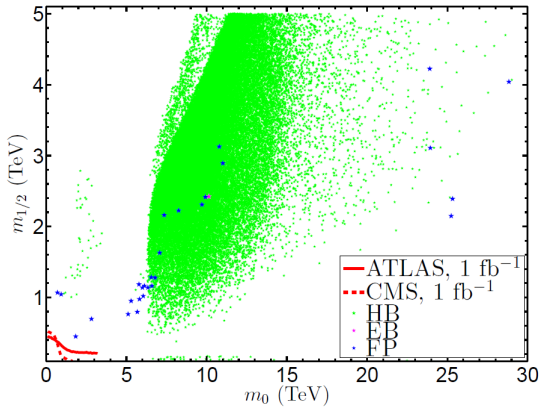


Focal Surface.



Akula, Liu, PN, Peim, PLB 709, 192 (2012), arXiv:1111.4589 [hep-ph]

Test of the hyperbolic geometry at the LHC for mSUGRA in view of the high Higgs boson mass



Mengxi Liu, PN: [arXiv:1213.7472\[hep-ph\]](https://arxiv.org/abs/1213.7472)

Path II:

Extra contributions to the Higgs boson mass

We consider an extra vector-like leptonic generation F consisting of L, L^c, E, E^c with $SU(3)_C \times SU(2)_L \times U(1)_Y$ quantum numbers

$$F : \quad \begin{array}{ll} L = (1, 2, -\frac{1}{2}), & E^c = (1, 1, 1), \\ L^c = (1, 2, +\frac{1}{2}), & E = (1, 1, -1). \end{array}$$

The superpotential for the vector-like leptonic supermultiplets is given by

$$W = y L H_d E^c + y' L^c H_u E + M_L L L^c + M_E E E^c + y_1^{(m)} L_3 H_d E^c + y_2^{(m)} L H_d E_3^c,$$

M_L and M_E are the vector-like masses and we assume that the extra leptons can decay only through the third generation particles.

The mixings ($y_{1,2}^{(m)}$) between the new leptons and $\hat{\tau}$ are assumed to be very small and they do not have any significant effect on the analysis here. Neglecting these small terms, the fermionic mass matrix now reduces to

$$M_F = \begin{pmatrix} M_L & \frac{1}{\sqrt{2}} y v_d \\ \frac{1}{\sqrt{2}} y' v_u & M_E \end{pmatrix}, \quad (5)$$

where the off-diagonal elements are the masses generated by Yukawa interactions while the diagonal elements are the vector masses. We call the heavier one τ'_1 and the lighter one τ'_2 .

Corrections to the Higgs mass

The Higgs potential is given by

$$V(H_u, H_d) = V_0 + \Delta V,$$

where ΔV is the correction to the effective potential at one-loop.

$$\Delta V = \frac{1}{64\pi^2} \text{Str} \left[M_i^4(H_u, H_d) \left(\ln \frac{M_i^2(H_u, H_d)}{Q^2} - \frac{3}{2} \right) \right], \quad (6)$$

where $\text{Str} = \sum_i c_i (2J_i + 1) (-1)^{2J_i}$ and $c_i (2J_i + 1)$ counts the degrees of freedom.

$$M_H^2 = \begin{pmatrix} M_Z^2 c_\beta^2 + M_A^2 s_\beta^2 + \Delta_{11} & -(M_Z^2 + M_A^2) s_\beta c_\beta + \Delta_{12} \\ -(M_Z^2 + M_A^2) s_\beta c_\beta + \Delta_{12} & M_Z^2 s_\beta^2 + M_A^2 c_\beta^2 + \Delta_{22} \end{pmatrix}, \quad (7)$$

where

$$M_Z^2 = \frac{1}{4} (g_1^2 + g_2^2) (v_u^2 + v_d^2), \quad M_A^2 = -2|B\mu|^2 / \sin(2\beta)$$

$$\Delta_{11} = \left(-\frac{1}{v_d} \frac{\partial}{\partial v_d} + \frac{\partial^2}{\partial v_d^2} \right) \Delta V, \quad (8)$$

$$\Delta_{22} = \left(-\frac{1}{v_u} \frac{\partial}{\partial v_u} + \frac{\partial^2}{\partial v_u^2} \right) \Delta V, \quad \Delta_{12} = \frac{\partial^2}{\partial v_u \partial v_d} \Delta V. \quad (9)$$

Contribution from the bosonic components of the vector multiplet ²⁹

To determine the contribution from the four super-partner fields of the vector-like fermions, one needs to find the mass eigenvalues of a 4×4 mass mixing matrix. In the basis $(\tilde{\tau}'_L, \tilde{\tau}'_R, \tau''_L, \tau''_R)$ it is given by

$$(M^2)_{4 \times 4} = \begin{pmatrix} (M_{\tilde{\tau}'}^2) & (M_{off}^2) \\ (M_{off}^2)^T & (M_{\tau''}^2) \end{pmatrix}, \quad (10)$$

where

$$(M_{\tilde{\tau}'}^2) = \begin{pmatrix} M_1^2 + \frac{1}{2} y^2 v_d^2 + M_L^2 + \frac{(g_1^2 - g_2^2)}{8} (v_d^2 - v_u^2) & \frac{1}{\sqrt{2}} y (A_{\tau'} v_d - \mu v_u) \\ \frac{1}{\sqrt{2}} y (A_{\tau'} v_d - \mu v_u) & M_1^2 + \frac{1}{2} y^2 v_d^2 + M_E^2 - \frac{g_1^2}{4} (v_d^2 - v_u^2) \end{pmatrix}$$

and

$$(M_{\tau''}^2) = \begin{pmatrix} M_2^2 + \frac{1}{2} y'^2 v_u^2 + M_L^2 - \frac{(g_1^2 - g_2^2)}{8} (v_d^2 - v_u^2) & \frac{1}{\sqrt{2}} y' (A_{\tau''} v_u - \mu v_d) \\ \frac{1}{\sqrt{2}} y' (A_{\tau''} v_u - \mu v_d) & M_2^2 + \frac{1}{2} y'^2 v_u^2 + M_E^2 + \frac{g_1^2}{4} (v_d^2 - v_u^2) \end{pmatrix}$$

where M_1, M_2 are soft scalar masses and

$$(M_{off}^2) = \begin{pmatrix} y' v_u M_L + y v_d M_E & 0 \\ 0 & y' v_u M_E + y v_d M_L \end{pmatrix}, \quad (13)$$

²⁹ W. -Z. Feng and PN, arXiv:1303.0289 [hep-ph].

Mass corrections from the bosonic sector

We assume that the soft masses are much larger than the vector masses. In this case we have $M_1^2, M_2^2 \gg M_L^2, M_E^2$ and the 4×4 mass² matrix factorizes to a product of two 2×2 matrices. The loop corrections from these to the scalar potential is given by

$$\Delta V^b = \Delta V_{\tilde{\tau}'}^b + \Delta V_{\tilde{\tau}''}^b.$$

$$\Delta V_{\tilde{\tau}'}^b = \frac{1}{64\pi^2} \sum_{i=1,2} 2m_{\tilde{\tau}'_i}^4 \left(\ln \frac{m_{\tilde{\tau}'_i}^2}{Q^2} - \frac{3}{2} \right),$$

$$\Delta V_{\tilde{\tau}''}^b = \frac{1}{64\pi^2} \sum_{i=1,2} 2m_{\tilde{\tau}''_i}^4 \left(\ln \frac{m_{\tilde{\tau}''_i}^2}{Q^2} - \frac{3}{2} \right).$$

The total contribution from the bosonic sector of the vector-like supermultiplets Δ_{ij}^b is

$$\Delta_{ij}^b = \Delta_{ij}^{\tilde{\tau}'} + \Delta_{ij}^{\tilde{\tau}''}. \quad (14)$$

Mass corrections from the fermionic sector

- The correction to the effective potential from vector like fermions is

$$\Delta V_{\tau'_{1,2}}^f = -\frac{1}{64\pi^2} \sum_{i=1,2} 4m_i^4 \left(\ln \frac{m_i^2}{Q^2} - \frac{3}{2} \right), \quad (15)$$

where $m_{1,2}$ are the mass eigenvalues of the vector-like fermions. Vector like fermions receive their masses from two sources: from the assumed vector masses and from the Yukawa couplings. The corrections from these are rather complicated. However, in the limit

$$m_1 \rightarrow \frac{1}{\sqrt{2}} y' v_u, \quad m_2 \rightarrow \frac{1}{\sqrt{2}} y v_d$$

the corrections have the following reduction.

$$\Delta_{11}^f = -\beta y^4 v_d^2 \ln \frac{y^4 v_d^4}{4Q^4}, \quad \Delta_{22}^f = -\beta y'^4 v_u^2 \ln \frac{y'^4 v_u^2}{4Q^4}, \quad \Delta_{12}^f = 0. \quad (16)$$

- The total result is the sum of the bosonic and the fermionic contributions and the Q dependence drops out.

$$\Delta_{ij} = \Delta_{ij}^b + \Delta_{ij}^f$$

Diphoton rate in SM

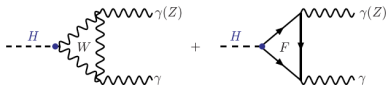
We first consider the Standard Model case with the Higgs doublet $H^T = (H^+, H^0)$ and the interaction Lagrangian

$$-\mathcal{L}_{\text{int}} = g_{hVV} h V_\mu^+ V^{-\mu} + g_{hff} h f \bar{f} + g_{hSS} h S \bar{S}$$

V, f, S denote vectors, fermions, and scalars, and $H^0 = (v + h)/\sqrt{2}$ and $v = 246$ GeV. At the one-loop level involving the exchange of spin 1, spin 1/2 and spin 0 particles in the loops the $h \rightarrow \gamma\gamma$ decay width is

$$\Gamma(h \rightarrow \gamma\gamma) = \frac{\alpha^2 m_h^3}{1024\pi^3} \left| \frac{g_{hVV}}{m_V^2} Q_V^2 A_1(\tau_V) + \frac{2g_{hff}}{m_f} N_{c,f} Q_f^2 A_{\frac{1}{2}}(\tau_f) + \frac{g_{hSS}}{m_S^2} N_{c,S} Q_S^2 A_0(\tau_S) \right|^2.$$

Q, N are charges and colors, A 's are the loop functions and $\tau_i = 4m_i^2/m_h^2$.



For the Standard Model

$$g_{hWW} = g_2 M_W, \quad g_{hff} = g_2 m_f / (2M_W)$$

For the SM diphoton contributions arise from the W and exchanges

$$\Gamma_{\text{SM}}(h \rightarrow \gamma\gamma) \approx \frac{\alpha_{em}^2 m_h^3}{256v^2 \pi^3} \left| A_1(\tau_W) + N_c Q_t^2 A_{\frac{1}{2}}(\tau_t) \right| \rightarrow \frac{\alpha_{em}^2 m_h^3}{256v^2 \pi^3} |\mathcal{A}_{\text{SM}}|^2,$$

and $\mathcal{A}_{\text{SM}} \approx -6.49$.

The loop functions $A_1(x)$, $A_{\frac{1}{2}}(x)$ and $A_0(x)$ are defined by

$$A_1(\tau) = -[2 + 3\tau + 3\tau(2 - \tau)f(\tau)], \quad (17)$$

$$A_{\frac{1}{2}}(\tau) = 2\tau[1 + (1 - \tau)f(\tau)], \quad (18)$$

$$A_0(\tau) = -\tau[1 - \tau f(\tau)]. \quad (19)$$

where the function $f(\tau)$ is given by

$$f(\tau) = \begin{cases} \left(\arcsin \frac{1}{\sqrt{\tau}}\right)^2, & \tau \geq 1; \\ -\frac{1}{4} \left[\ln \frac{\eta_+}{\eta_-} - i\pi\right]^2, & \tau < 1. \end{cases} \quad (20)$$

where $\eta_{\pm} \equiv (1 \pm \sqrt{1 - \tau})$ and $\tau = 4m^2/m_h^2$ for a particle running in the loop with mass m . For the case when $\tau \gg 1$ one has

$$f(\tau) \rightarrow \frac{1}{\tau} \left(1 + \frac{1}{3\tau} + \frac{3}{20\tau^2} + \dots\right), \quad (21)$$

and in this limit $A_1 \rightarrow -7$, $A_{\frac{1}{2}} \rightarrow 4/3$, $A_0 \rightarrow 1/3$.

A partial list of some earlier works on diphoton rate and mass corrections

- M. Carena, S. Gori, N. R. Shah and C. E. Wagner, JHEP 1203, 014 (2012), arXiv:1112.3336 [hep-ph].
- M. Carena, I. Low and C. E. Wagner, JHEP 1208, 060 (2012), arXiv:1206.1082 [hep-ph].
- L. G. Almeida, E. Bertuzzo, P. A. Machado and R. Z. Funchal, JHEP 1211, 085 (2012), arXiv:1207.5254 [hep-ph].
- J. Kearney, A. Pierce and N. Weiner, Phys.Rev. D86, 113005 (2012), arXiv:1207.7062 [hep-ph].
- G. F. Giudice, P. Paradisi and A. Strumia (2012), arXiv:1207.6393 [hep-ph].
- H. Davoudiasl, H.-S. Lee and W. J. Marciano, Phys.Rev. D86, 095009 (2012), arXiv:1208.2973 [hep-ph].
- A. Joglekar, P. Schwaller and C. E. Wagner (2012), arXiv:1207.4235 [hep-ph].
- N. Arkani-Hamed, K. Blum, R. T. D'Agnolo and J. Fan (2012), arXiv:1207.4482 [hep-ph].
- H. An, T. Liu and L.-T. Wang (2012), arXiv:1207.2473 [hep-ph].

Heavy particles in the loop

If the masses of the particles running in the loops which give rise to the decay of the Higgs to diphoton, are much heavier than the Higgs boson, the decay of $h \rightarrow \gamma\gamma$ is governed by an $h\gamma\gamma$ effective coupling³⁰

$$\mathcal{L}_{h\gamma\gamma} = \frac{\alpha_{em}}{16\pi} h \left[\sum_i b_i \frac{\partial}{\partial v} \log m_i^2(v) \right] F_{\mu\nu} F^{\mu\nu} .$$

where b_i are:

$$\begin{aligned} b_1 &= -7Q_V^2, & \text{for a vector boson,} \\ b_{\frac{1}{2}} &= \frac{4}{3}Q_f^2, & \text{for a Dirac fermion,} \\ b_0 &= \frac{1}{3}Q_S^2, & \text{for a charged scalar.} \end{aligned}$$

When there are multiple particles carrying the same electric charge circulating in the loops, one can write a more general expression by replacing $\log m_i^2$ by $\log (\det M^2)$, where M^2 is the mass² matrix of the particles circulating in the loops.

Extension to SUSY

For MSSM one has two Higgs doublets:

$$H_d = \begin{pmatrix} H_d^0 \\ H_d^- \end{pmatrix} = \begin{pmatrix} \frac{v_d + \phi_1}{\sqrt{2}} \\ H_d^- \end{pmatrix}, \quad H_u = \begin{pmatrix} H_u^+ \\ H_u^0 \end{pmatrix} = \begin{pmatrix} H_u^+ \\ \frac{v_u + \phi_2}{\sqrt{2}} \end{pmatrix}.$$

v_d and v_u are the VEVs of H_d^0 and H_u^0 . The effective Higgs coupling in this case is

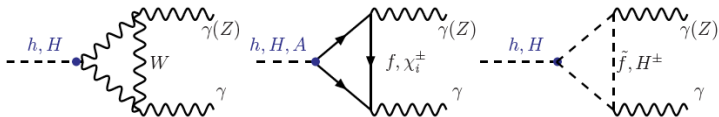
$$\mathcal{L}_{h\gamma\gamma}^{\text{SUSY}} = \frac{\alpha_{em}}{16\pi} h \sum_i b_i \left[\cos \alpha \frac{\partial}{\partial v_u} \log m_i^2(v_u) - \sin \alpha \frac{\partial}{\partial v_d} \log m_i^2(v_d) \right] F_{\mu\nu} F^{\mu\nu}.$$

α is the mixing angle between the two CP-even Higgs in the MSSM. The diphoton decay width in this case is

$$\begin{aligned} \Gamma_{\text{SUSY}}(h \rightarrow \gamma\gamma) \approx & \frac{\alpha_{em}^2 m_h^3}{256 v^2 \pi^3} \left| \sin(\beta - \alpha) Q_W^2 A_1(\tau_W) + \frac{\cos \alpha}{\sin \beta} N_t Q_t^2 A_{\frac{1}{2}}(\tau_t) \right. \\ & + \frac{b_1 v}{2} \left(\cos \alpha \frac{\partial}{\partial v_u} \log m_f^2 - \sin \alpha \frac{\partial}{\partial v_d} \log m_f^2 \right) N_f Q_f^2 \\ & \left. + \frac{b_0 v}{2} \left(\cos \alpha \frac{\partial}{\partial v_u} \log m_S^2 - \sin \alpha \frac{\partial}{\partial v_d} \log m_S^2 \right) N_{c,S} Q_S^2 \right|^2. \end{aligned}$$

Compared to the Standard Model case, the Higgs couplings to the W boson and to the top quark are modified by factors $\sin(\beta - \alpha)$ and $\frac{\cos \alpha}{\sin \beta}$. Now the fermionic contribution also comes from the chargino exchange while the scalar contribution includes contributions from the exchange of the sleptons, the squarks and the charged Higgs fields.

Higgs to diphoton decay in SUSY



In SUSY the Higgs to diphoton decay proceeds via exchange of W , t and via exchange of charginos, sfermions and charged Higgs. We will ignore these usual SUSY contributions and consider only the contributions from the exchange of the vector multiplet.

Contribution from the fermionic components of the vector multiplet to the diphoton rate

If the contribution is only from the vector-like fermions, the Higgs diphoton rate is enhanced by a factor of:

$$\frac{\Gamma(h \rightarrow \gamma\gamma)}{\Gamma(h \rightarrow \gamma\gamma)_{SM}} \approx \left| 1 + \frac{1}{\mathcal{A}_{SM}} b_{\frac{1}{2}} N_f Q_f^2 \frac{-v^2 y y'}{2m_1 m_2} \cos(\alpha + \beta) \right|^2 \quad (23)$$

$$\approx \left| 1 + 0.1 N_f \frac{v^2 y y'}{m_1 m_2} \cos(\alpha + \beta) \right|^2 \equiv |1 + r_f|^2. \quad (24)$$

We consider the limit $M_1, M_2 \gg M_L, M_E$. In this limit the total bosonic contribution can be measured by r_b , which reads

$$r_b = r_1 + r_2 \equiv \frac{1}{\mathcal{A}_{\text{SM}}} \frac{b_0 v}{2} (\Xi_1 + \Xi_2), \quad (25)$$

where

$$\Xi_1 = \cos \alpha \frac{\partial}{\partial v_u} \log(\det M^2) - \sin \alpha \frac{\partial}{\partial v_d} \log(\det M^2), \quad (26)$$

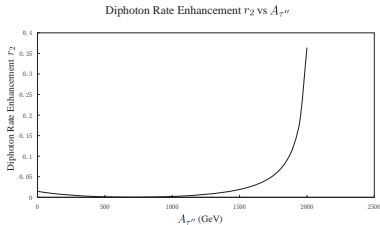
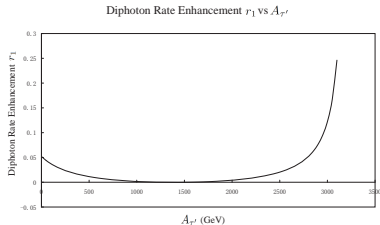
$$\Xi_2 = \cos \alpha \frac{\partial}{\partial v_u} \log(\det M'^2) - \sin \alpha \frac{\partial}{\partial v_d} \log(\det M'^2). \quad (27)$$

Ξ_1 arises from $\tilde{\tau}'$ mass² matrix. A direct computation gives

$$\Xi_1 = \frac{1}{m_{\tilde{\tau}'_1}^2 m_{\tilde{\tau}'_2}^2} \left\{ \left[\frac{1}{2} g_1^2 M_{11}^2 - \frac{(g_1^2 - g_2^2)}{4} M_{22}^2 \right] v \sin(\alpha + \beta) + \sqrt{2} M_{12}^2 y(A_{\tau'}) \sin \alpha + \mu \cos \alpha \right\}.$$

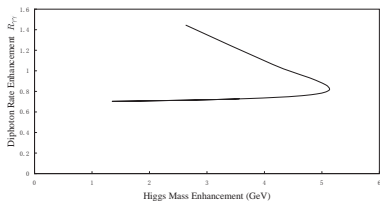
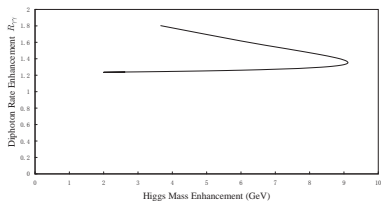
Ξ_2 arises from $\tilde{\tau}''$ mass² matrix.

$$\Xi_2 = \frac{1}{m_{\tilde{\tau}''_1}^2 m_{\tilde{\tau}''_2}^2} \left\{ \left[-\frac{1}{2} g_1^2 M_{11}'^2 + \frac{(g_1^2 - g_2^2)}{4} M_{22}'^2 \right] v \sin(\alpha + \beta) - \sqrt{2} M_{12}'^2 y'(A_{\tau''}) \cos \alpha + \mu \sin \alpha \right\}.$$



An analysis of the diphoton rate enhancement (top panels) and enhancement of the Higgs boson mass (bottom panels) for the case when the vector masses vanish, i.e., $M_L = M_E = 0$. Left top: A plot of the diphoton rate enhancement r_1 (from $\tilde{\tau}'_{1,2}$) vs $A_{\tau'}$; Right top: A plot of the diphoton rate enhancement r_2 (from $\tilde{\tau}''_{1,2}$) vs $A_{\tau''}$. Left bottom: A plot of the Higgs mass enhancement from $\tilde{\tau}'$ sector (GeV) vs $A_{\tau'}$; Right bottom: A plot of the Higgs mass enhancement from $\tilde{\tau}''$ sector (GeV) vs $A_{\tau''}$.

W. -Z. Feng and P. N, arXiv:1303.0289 [hep-ph].

Diphoton Rate Enhancement $R_{\gamma\gamma}$ vs Higgs Mass EnhancementDiphoton Rate Enhancement $R_{\gamma\gamma}$ vs Higgs Mass Enhancement

Left panel: A display of the correlation between the Higgs diphoton rate enhancement and the Higgs mass enhancement in the decoupled limit where $M_L = M_E = 0$ as in Fig. 2. Right panel: A display of the correlation between the Higgs diphoton rate enhancement and the Higgs mass enhancement for the case when the vector masses are non-vanishing where $M_L = M_E = 210$ GeV. The two branches shown in each of the two plots are due to the rise and fall of the Higgs mass enhancement as exhibited in the lower panel of Fig. 2 and 4.

W. -Z. Feng and P. N, arXiv:1303.0289 [hep-ph].

Constraints on new particles by electroweak precision tests

- L. G. Almeida, E. Bertuzzo, P. A. Machado and R. Z. Funchal, JHEP 1211, 085 (2012), arXiv:1207.5254 [hep-ph].
- A. Joglekar, P. Schwaller and C. E. Wagner (2012), arXiv:1207.4235 [hep-ph].
- N. Arkani-Hamed, K. Blum, R. T. D'Agnolo and J. Fan (2012), arXiv:1207.4482 [hep-ph].
- S. P. Martin, Phys.Rev. D82, 055019 (2010), arXiv:1006.4186 [hep-ph].
- G. Cynolter and E. Lendvai, Eur.Phys.J. C58, 463 (2008), arXiv:0804.4080 [hep-ph].
- Detection of new particles: S. B. Giddings, T. Liu, I. Low and E. Mintun (2013), arXiv:1301.2324 [hep-ph].

Unification and Proton decay

- Unification leads to an explanation of the three coupling constants $\alpha_1, \alpha_2, \alpha_3$ in terms of a single coupling at the GUT scale.
- Quantization of charge

$$\left| 1 + \frac{Q_e}{Q_p} \right| < O(10^{-21}).$$

- Quark lepton unification.
- Proton decay is a consequence of quark -lepton unification .
 - 4 D GUTs
 - 5 D and 6D models
 - string and D brane models

Why proton decay is of great importance for fundamental physics.

The main points about proton decay are

- Observation of proton decay will test the basic idea of quark-lepton unification, i.e., that they are members of the same common multiplet. This phenomenon is not testable in any other low energy process.
- It will probe length scales which are extra-ordinarily small, i.e., $O(10^{-33})\text{m}$.
- Proton decay can provide a test for supersymmetry: In supersymmetry the dominant mode is typically $p \rightarrow \bar{\nu} K^+$ and its observation will give support to the existence of SUSY at the fundamental level.
- Proton decay in principle can provide clues to the existence of strings and possibly of extra dimensions.
- Proton decay can provide a clue to the possible origin of matter generations.

Classification of proton decay operators

- The classification of p decay from higher dimensional operators consistent with the SM gauge group was done early on by Weinberg and by Wilczek, Zee³¹.
- There are two principle ways in which baryon and lepton number violating dimension six operators can arise in grand unified theories and in unified models based on strings and branes. These are
 - Via exchange of lepto-quarks: Valid for both non-supersymmetric as well as for supersymmetric grand unified theories.
 - Via exchange of Higgsino triplets. This is specific to SUSY models.

³¹S. Weinberg, PRL 43, 1566(1979); F. Wilczek and A. Zee, PRL 43, 1571(1979)

Proton decay from Lepto-quark exchange

- For dim 6 operators arising from lepto-quark exchange the dominant decay mode is $p \rightarrow e^+ \pi^0$ and is predicted to have a lifetime³²

$$\tau_p(p \rightarrow \pi^0 e^+) = C_p \times 1.6 \times 10^{36} \text{yrs} \left(\frac{M_X}{2 \times 10^{16} \text{GeV}} \right)^4 \quad (30)$$

where C_p is model dependent but $O(1)$.

- In D-branes (Klebanov-Witten) the decay lifetime is

$$\tau_{st}(p \rightarrow e^+ \pi^0) = \tau_{GUT}(p \rightarrow e^+ \pi^0) C_{st} \frac{M_G^4}{M_X^4}$$

where C_{st} is the string enhancement factor and estimates give $C_{st} = 0.5 - 1.2$. The dominant process is $p \rightarrow e_L^+ \pi^0$ while the decay $p \rightarrow e_R^+ \pi^0$ is suppressed.

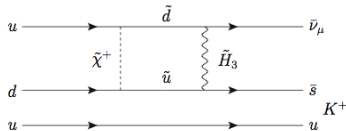
- The current experimental limit is

$$\tau_p(p \rightarrow e^+ \pi^0) > 1.4 \times 10^{34} \text{yrs.}$$

³²p lifetime is sensitive to fermion mixing: P. Fileviez Perez, PLB 595, 476 (2004).

Proton decay via triplet Higgsino exchange: $p \rightarrow \bar{\nu} K^+$ mode

Operators arising from triplet Higgsino exchange must be dressed by charginos, neutralinos and gluino exchanges to produce B&L violating dim 6 operators. All these dressings have been computed fully³³. The dim 5 proton decay has a significant model dependence. Both high energy and low energy physics affect this decay³⁴. There is a rich literature on dim 5 decay³⁵



Dressing loop diagrams for $p \rightarrow \bar{\nu} K^+$ decay from dimension five operators via exchange of chargino's, squarks and Higgsino color triplets.

Very crudely

$$\tau(p \rightarrow \bar{\nu} K^+) \simeq C(m_{\tilde{q}}^4 M_{\tilde{H}_3}^2 / m_{\tilde{\chi}^\pm}^2 \tan^2 \beta)$$

For $m_{\tilde{q}}$ in the sub TeV region, this could lead to too short a lifetime for this mode. This is specifically the case for "natural models" which advocate $M_s \sim 300 - 500$ GeV.

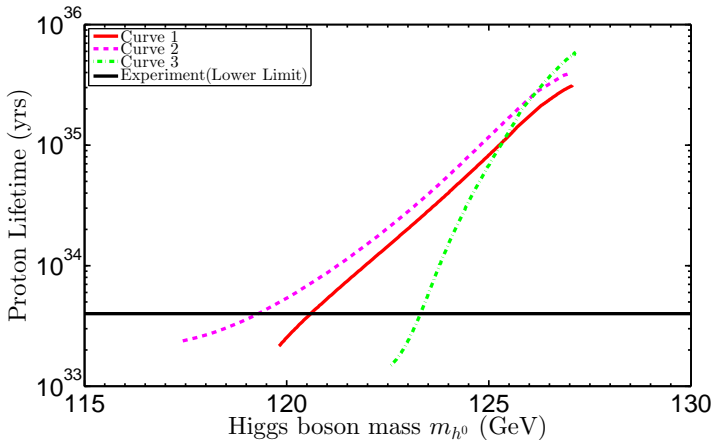
³³ Arnowitt, Chamseddine, PN; Hisano, Murayama, Yanagida; Lucas, Raby; Goto, Nihei . . .

³⁴ See, e.g., PN, P Fileviez Perez, Phys. Report, Vol. 441, No.5-6,(2007).

³⁵ Weinberg; Sakai, Yanagida; Dimopoulos, Raby Wilczek; Ellis, Nanopoulos, Rudaz; Arnowitt, PN; Babu, Pati, Wilczek; Bajc, Fileviez Perez, Senjanovic; Dosner; Dermisek, Mafi, Raby; Emmanuel-Costa, Wiesenfeldt; Dutta, Mimura, Mohapatra; Syed, PN; Babu, Pati, Tavartkiladze, . . .

Implications of the high Higgs mass for proton stability

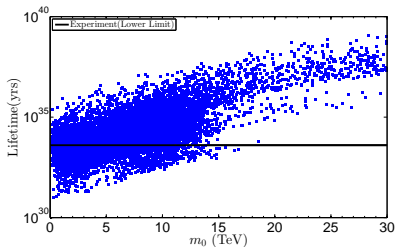
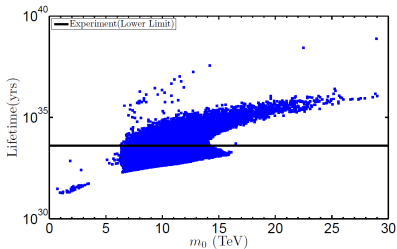
Mengxi Liu, PN: arXiv:1303.7472



A 5-10 GeV shift in the Higgs boson mass can result in a shift in the proton decay life time for the mode $\bar{\nu}K^+$ by up to 2 orders of magnitude.

$\tau_{exp}(p \rightarrow \bar{\nu}K^+)$ constraint on the SUGRA parameter space

Mengxi Liu, PN: arXiv:1303.7472



$p \rightarrow \bar{\nu}K^+$ lifetime constraint on mSUGRA/CMSSM (left panel) and on non-universal SUGRA model with gaugino mass non-universalities (right panel) where $M_{H_3}^{eff}/M_G = 50$.

What about fine tuning?

- **REWSB:** Fine tuning in REWSB arises from the equation that determines the Z -boson mass

$$\frac{1}{2}M_Z^2 = -\mu^2 + |m_{H_u}|^2 + \dots$$

If μ or $|m_{H_u}|$ get too large, one needs a fine tuning to get the Z mass. An obvious ways to define fine tuning in REWSB is³⁶

$$F_{rewsb} \sim \frac{2|m_{H_u}|^2}{M_Z^2}$$

Now $F_{rewsb} \sim m_0^2$


- **Proton decay:** Here we define fine tuning as

$$F_{pd} = \frac{4 \times 10^{33} \text{yr}}{\tau(p \rightarrow \bar{\nu} K^+) \text{yr}}. \quad (31)$$

F_{pd} behaves like $F_{pd} \sim 1/m_0^4$. A more appropriate object to consider then is

$$\mathcal{F} = \left(\prod_{i=1}^n F_i \right)^{\frac{1}{n}}. \quad (32)$$

In this circumstance $\mathcal{F} \sim 1/m_0^2$, i.e., a smaller fine tuning occurs at a larger m_0 .


³⁶This also follows from $F = (a/f(a)) \partial f / \partial a$, where \bar{a} is the sensitive 

Similar considerations apply if we consider EDMs in SUSY ³⁷

$$d_e \sim 10^{-25} \text{ecm} \times \sin \phi \left(\frac{300 \text{GeV}}{m_0} \right)^2 \left(\frac{\tan \beta}{3} \right) < 1.0 \times 10^{-27} \text{ecm}.$$

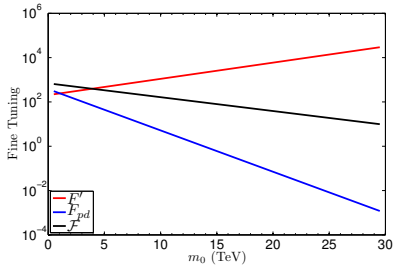
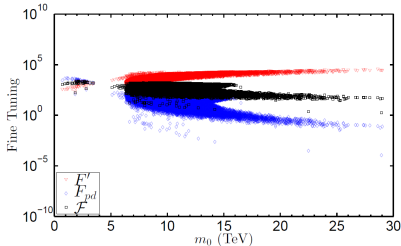
Here

$$F_{de} \sim 1/m_0^2.$$

³⁷FCNC processes along with EDMs have been considered by Jaeckel and Khoze, JHEP 1211, 115 (2012) [arXiv:1205.7091 [hep-ph]] with similar conclusions. 

Fine tunings with inclusion of p decay

Mengxi Liu, PN: arXiv:1303.7472

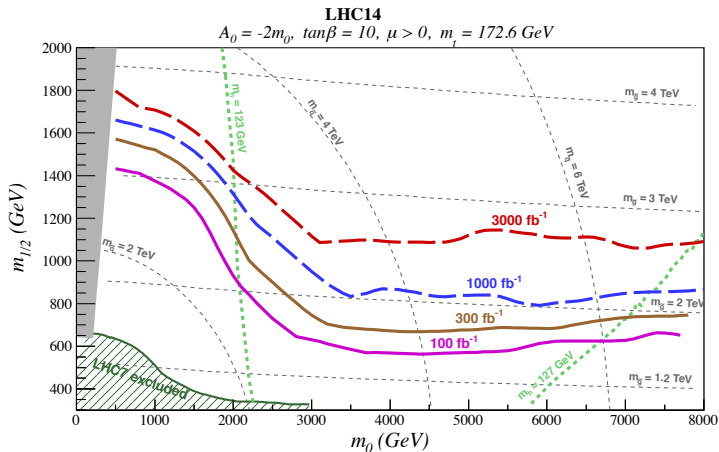


Top left: Fine tuning constraint from REWSB and from proton stability for the mode $p \rightarrow \bar{\nu}K^+$ and the mean as a function of m_0 for mSUGRA. Right: A smooth curve through the averages³⁸.

The combined fine tuning appears to favor larger m_0 .

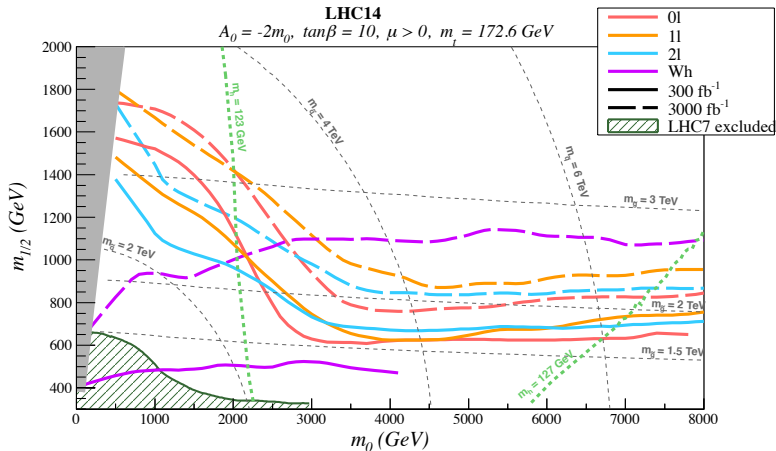
³⁸ The analysis is similar in spirit to a recent work (Jaeckel, Khoze, arXiv:1205.7091 [hep-ph]) where FCNC and CP violation were included along with REWSB in the analysis of fine tuning

Projected discovery reach in $m_0 - m_{1/2}$ at $\sqrt{s} = 14$ TeV for mSUGRA



From H. Baer, V. Barger, A. Lessa and X. Tata, Phys.Rev. D86 (2012) 117701, arXiv:1207.4846 [hep-ph].

Projected discovery reach in $m_0 - m_{1/2}$ at $\sqrt{s} = 14$ TeV for mSUGRA



From H. Baer, V. Barger, A. Lessa and X. Tata, Phys.Rev. D86 (2012) 117701
arXiv:1207.4846 [hep-ph].

The Higgs and the Standard Model

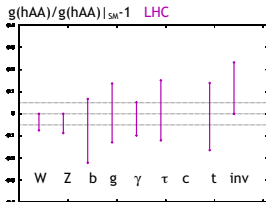
If the observed boson is a Higgs boson, its couplings with fermions has the relation

$$h_{hff} \sim m_f/v.$$

Additionally of course the couplings of the Higgs with gauge fields are determined by gauge invariance. Thus the test of SM will come by testing all the couplings, i.e., couplings to fermion-anti-fermion pairs and to dibosons

$$hf\bar{f}, hWW, hZZ, h\gamma\gamma, hZ\gamma.$$

- How well can we check the couplings? At LHC with $\sqrt{s} = 14$ TeV, and $\mathcal{L} = 300 \text{ fb}^{-1}$ one could attain up to 10% accuracy for coupling of h with gauge bosons and up to $\sim 20\%$ for couplings to b, τ and t.

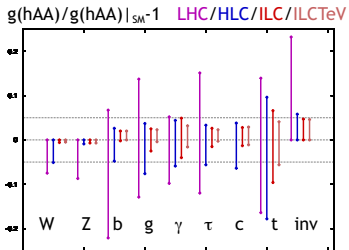


From: M. Peskin arXiv:1207.2516

The marked horizontal band represents a 5% deviation from the Standard Model prediction for the coupling.

Sensitivities for the measurement of the Higgs couplings at LHC vs ILC

- A comparison of LHC vs ILC



Taken from: M. Peskin arXiv:1207.2516

- (i) 'HLC': ILC at 250 GeV and 250 fb^{-1} ; (ii) ILC: 500 GeV with 500 fb^{-1} , (iii) ILC TeV: 1000 fb^{-1} for an upgraded ILC at 1 TeV.
- The $h\gamma\gamma$ and $h\gamma Z$ could provide a faster route to discovery of new physics because both the standard model contribution and the SUSY or new physics contributions also arise at the loop level.

Conclusion

- The high value of the Higgs boson mass contains clues to the possible origin of new physics. Combined with the result from the muon anomalous magnetic moment, the number of options narrow.
- We investigated two avenues to resolve the conflict: One possibility is that there is an additional source to the Higgs boson mass, outside of MSSM, such as contribution from vector like multiplets. Their contribution lowers the SUSY scale resolving the conflict.
- The second possibility is that if one stays within MSSM, then a split scale SUSY can explain the two experiments which appear to be in conflict. The split scale consists of one heavy scale for color particles to explain the Higgs boson mass, and a second light scale for uncolored particles to explain $g_\mu - 2$. The split scale SUSY arises naturally in \tilde{g} SUGRA model where radiative breaking of the electroweak symmetry is driven by the gluino mass.
- Further, data from LHC should allow one to discriminate among these and other options.